atmosphere

MDPI

Article

Experimental Research on Permeability and Effective Radon Reduction of Chemical Solidification of Uranium Tailings

Jindong Wang [1] and Shuai Zhang [2,3,*]

[1] College of Energy Engineering, Yulin University, Yulin 719000, China; wjd1593572024@163.com
[2] College of Energy Science and Engineering, Xi'an University of Science and Technology, Xi'an 710054, China
[3] School of Resources and Safety Engineering, University of South China, Hengyang 421001, China
* Correspondence: zhangshuai@xust.edu.cn

Abstract: To be able to study the permeability coefficient and radon reduction effect of three materials before and after the solidification of uranium tailings. Firstly, uranium tailings, blast furnace slag, lime, fly ash and cement were selected as raw materials for the experiment. Three solidified materials were mixed with 7.5%, 10% and 12.5% of equal proportions of cement. The curing samples of nine kinds of solidified bodies were prepared after curing. Subsequently, the permeability coefficient was determined through the utilization of X-ray diffraction (XRD) and scanning electron microscopy (SEM). And cumulative radon concentrations in uranium tailings and samples were measured by RAD7. Thus, the radon exhalation rate of the original sample and the sample were determined. The experimental results show that the permeability coefficient of nine samples decreased with the quadratic function with the increase in the amount of curing agent. Microscopic scanning results show that there is a positive correlation among the radon exhalation rate, permeability coefficient and cementation degree. The best material for solidifying uranium tailings and radon insulation was blast furnace slag, followed by fly ash.

Keywords: uranium tail sand; curing base; waste utilization; permeability coefficient; radon exhalation rate

Citation: Wang, J.; Zhang, S. Experimental Research on Permeability and Effective Radon Reduction of Chemical Solidification of Uranium Tailings. *Atmosphere* **2024**, *15*, 1493. https://doi.org/10.3390/atmos15121493

Academic Editor: Boris Igor Palella

Received: 13 September 2024
Revised: 24 November 2024
Accepted: 3 December 2024
Published: 14 December 2024

Uranium tailings are produced after a series of hydrometallurgical processes such as solid–liquid separation and ion exchange or extraction from uranium ore [1]. These processes are used to extract uranium from ore, resulting in a large amount of waste material containing residual radioactive material, known as uranium tailings. Uranium tailings often contain a small amount of unextracted uranium and other radioactive elements, which need to be effectively treated. It includes the radioactive element radon (Rn), which is highly volatile and can penetrate through the soil layer to the surface, causing long-term harm to the environment and human health. Therefore, finding effective methods to solidify and stabilize uranium tailings and reduce radon emissions has become an important issue in the field of environmental engineering and nuclear safety. The progress of the nuclear industry has brought both new challenges and new opportunities. China's demand for uranium is expected to rise steadily as technological progress and nuclear energy become increasingly viable solutions for sustainable power generation. This growing demand for uranium is driven by the country's expanding nuclear energy infrastructure and its commitment to reducing carbon emissions through cleaner energy sources. According to incomplete statistics, the total amount of uranium tailings is about 20 billion tons, and the total amount of uranium waste rock is about 40 billion tons [2]. The huge content of uranium tailing waste residue contains a variety of radionuclides and is highly toxic. Nearly 30% of the radionuclides are long-lived radionuclides. For example, the half-life of ^{238}U is 4.51×10^9 years, the half-life of ^{230}Th is 7.7×10^7 years, and the half-life of ^{226}Ra is 1.6×10^3 years [3]. These nuclides will bring potential radiation damage to the natural environment. In addition, a study also showed that the curing effect is affected by a variety of process parameters, such as the type of curing agent, dosage, curing temperature and

curing time. These parameters not only affect the mechanical properties of the solidified body but also significantly affect its radioactive shielding effect. In order to optimize the curing process, researchers used a series of characterization techniques, such as X-ray diffraction (XRD), scanning electron microscopy (SEM) and thermogravimetric analysis (TGA), to reveal the physical and chemical changes that occurred during the curing process so as to guide the optimization of process parameters.

At present, for uranium tailings, the curing technology developed and popularized at home and abroad mainly includes cement curing and asphalt curing [4]. However, in considering the implementation means and economic benefits and other factors, there will be many inconveniences in the practical application of the process. Cement curing has the disadvantages of a high capacity and nuclide leaching rate and high economic costs. The curing operation of asphalt is complex, easily produces secondary pollution and has poor long-term stability. Blast furnace slag (GBFS), quicklime (QL) and fly ash (FA) for soft soil solidification research and application in engineering practice are also more successful. Based on the most basic hydration mechanism of GBFS, Wu et al. [5] deeply analyzed the chemical composition and structural characteristics of GBFS and described the reasons for the potential activity of GBFS. Yi Yaolin et al. [6] deeply discussed the theoretical basis of granulated blast furnace slag replacing or partially replacing cement from the source and composition of blast furnace slag, as well as its application in soil reinforcement and curing mechanism. Aly Ahmed et al. [7] analyzed the microstructure of the solidified body after scanning the materials such as granulated blast furnace slag, fly ash and gypsum. Laxmikant Yadu et al. [8–11] described and characterized the macroscopic (mechanical compressive strength) characteristics of fly ash and other materials. Therefore, this study aimed to explore the main factors affecting the radon exhalation rate and establish the relationship between the microstructure characteristics, permeability coefficient and radon exhalation rate. Based on the detailed analysis of the properties of uranium tailings, the permeability coefficient, scanning results and radon exhalation rate of uranium tailings solidified with blast furnace slag, quicklime and fly ash were studied so as to reveal the relationship among the radon exhalation rate, permeability coefficient, and scanning results.

1. Test Materials and Preparation

1.1. Testing Material

The uranium tailings used in this study were taken from a uranium tailing pond. The main chemical composition is shown in Table 1, which is granular soil yellow, with black particles in the middle. Uranium tailings mainly come from the traditional heap leaching process of uranium ore. Uranium tailings were placed in a blast drying oven (105 °C, 24 h). After natural cooling, a small amount of original tailings were taken for mineral phase and morphology analysis, and the remaining tailings were sealed for subsequent use.

Table 1. Data of chemical composition for uranium tailing samples after normalizing (wt%).

Chemical Composition	SiO_2	Fe_2O_3	Al_2O_3	MgO	MnO	CaO	P_2O_5	FeO	K_2O	U
Mass fraction/%	85.25	1.63	6.18	0.078	0.007	0.161	0.082	0.36	3.18	0.006

Blast furnace slag is obtained through the rapid cooling of blast furnace slag produced in the process of smelting pig iron, and S105 (the activation index reaches 105% after 28 days) grade material is obtained through online purchase. The main chemical composition of blast furnace slag is shown in Table 2. Lime is a white massive or granular object, the main component of which is CaO, and its content is not less than 98% after burning loss. The fly ash was taken from the main solidified waste discharged from the coal-fired power plant Huadian Xinzhou Guangyu Coal Power Co., Ltd. (Xinzhou, China), and its main chemical

composition is shown in Table 3. The cement was P.O 42.5 cement produced by Conch Cement Co., Ltd. (Wuhu, China).

Table 2. Main chemical composition of granulated blast furnace slag (GBFS) (wt%).

Chemical Composition	CaO	SiO_2	Al_2O_3	MgO	S	FeO	MnO
Mass fraction/%	31–50	31–44	6–18	1–16	0.2–2	0.2–1.5	0.05–2.6

Table 3. Chemical composition of fly ash (wt%).

Chemical Composition	SiO_2	Al_2O_3	Fe_2O_3	FeO	CaO	TiO_2	Miscellaneous
Mass fraction/%	56.51	24.7	2.87	1.95	6.75	1.72	5.5

1.2. Testing Equipment

This test included the preparation of the sample and the scanning results of the sample, and the determination of the permeability coefficient and radon exhalation rate. The equipment for sample preparation included a blast drying box (101-0 type), cement mixer (HJB type), shaking table (HJZ-1 type), curing box (YH-40B type), and air compressor (HK-200 type). The above equipment are from Jiangyan City, Jiangsu Province, Taizhou, Jiangsu Province. The later determination of the sample included an X-ray diffractometer (D8-Advance type) (Germany Bruker Company, Saarbrucken, Germany), field emission scanning electron microscope (Helios Nanolab 600i type) (Germany Bruker Company, Saarbrucken, Germany), uranium tailing gas–water infiltration experimental device (17058 type) (Xi'an Yongrui Jie Energy Technology Co., LTD., Xi'an China), and alpha energy spectrum radon detector (RAD7 type) (DURRIDGE, Billerica, MA, USA).

1.3. Preparation of Specimen

A reasonable ratio is the primary factor in determining the quality of the experiment. In considering various factors, materials such as uranium tailings (aggregate and radium source), blast furnace slag (cement), quicklime (cement), fly ash (cement) and cement (cement) were selected. Now, according to the relevant literature on filling bodies and soft soil [5,12,13], the pertinent research findings are presented in tabular form (see Table 4), and the ratio of uranium tailing solidification was calculated.

Table 4. Curing test ratio table.

Sample Name	Mix Proportion
	Cement–Curing Agent–Uranium Tailings
GBFS-1	1:1:11.3
GBFS-2	1:1:8
GBFS-3	1:1:6
QL-1	1:1:11.3
QL-2	1:1:8
QL-3	1:1:6
FA-1	1:1:11.3
FA-2	1:1:8
FA-3	1:1:6

Note: The water–cement ratio of the test was 0.33. gBFS indicates that the sample was mixed with blast furnace slag, while QL indicates that the sample was mixed with quicklime. FA indicates that the sample was mixed with fly ash.

Based on the calculated mix ratio, the quantities of uranium tailings, blast furnace slag, lime, fly ash, cement and water were precisely measured using a precision balance. These materials were then combined and thoroughly mixed in a mechanical mixer to ensure a uniform distribution of components. Following the mixing process, solidified uranium tailings were formed using a shaking table to achieve the desired compaction and consistency. The mixture was then transferred to a demolding machine to remove it from the molds and subsequently placed in a curing box for controlled setting and hardening. This process ensured that the solidified tailings had consistent quality and structural integrity. The preparation of the sample consisted of four steps. First, the required mass of each material was calculated according to the specified mix ratio. This included uranium tailings, blast furnace slag (or quicklime or fly ash), cement and water. Concurrently, the test mold was thoroughly cleaned and evenly coated with oil to facilitate easy demolding later. In the second step, the measured uranium tailings, blast furnace slag (or quicklime or fly ash) and cement were added to a mechanical mixer. The dry materials were mixed thoroughly until they were evenly distributed. Water was then gradually added to the mixture, which was stirred continuously until the resulting wet material achieved a mortar slurry with appropriate fluidity. The wet mixture was poured into the prepared test mold, which had been coated with oil. The mold was then placed on a vibrating table to ensure that all air bubbles were removed and the material was evenly distributed. The filled mold was left in a cool place for 24 h to allow the initial setting of the material. After 24 h, the sample was carefully demolded and labeled. The specimens were then transferred to a curing box, where they were maintained at a temperature of 20 $\pm$ 2 °C and a relative humidity of greater than 95% for 28 days. During this curing period, the permeability coefficient and cumulative radon concentration of the sample were measured and recorded for subsequent experiments. This detailed process ensured that the samples achieved the necessary consistency and properties for accurate testing and evaluation.

2. Sample Determination Method

2.1. Permeability Coefficient

The seepage coefficient of a solidified uranium tailing body is a critical indicator that measures the seepage capacity of uranium tailings after they have been solidified. This coefficient reflects how easily fluids can pass through the solidified material, which is essential for evaluating the effectiveness of the solidification process in preventing the migration of potentially harmful substances. A lower seepage coefficient indicates better containment and lower risk of leakage, thereby ensuring enhanced environmental safety and protection against the spread of contaminants. This parameter is crucial for assessing the long-term stability and integrity of the solidified tailings and for making informed decisions about their management and disposal. Its physical meaning is the permeability of the medium to a specific fluid. Through the gas–water permeability test device of uranium tailings, the liquid flow rate and pressure value of the uranium tailings' solidified body were measured, and then the permeability coefficient was obtained according to Darcy's law formula, and the relationship between the permeability coefficient and the strength and content of the uranium tailings samples was studied. The calculation method of the permeability coefficient of the uranium tailing sample is as follows:

$$K = \frac{Q \cdot L}{S \cdot H \cdot T} \tag{1}$$

In Formula (1), K represents the permeability coefficient at the test temperature of 23 °C, cm·s^{-1}; Q is the amount of water exuded within 15 min when the high pressure value at the inlet of the sample tends to be balanced, cm^3; L is the length of the specimen, cm; S represents the cross-sectional area, cm^2; H represents the difference in water level (in accordance with the height of the sample), cm; and T represents the test time, s.

2.2. Radon Exhalation Rate

In accordance with the diffusion and migration law of radon [14], the principle of the RAD7 radon detector [15], the closed cavity method and the theoretical model [16] in the relevant literature, the measured values of the unilateral and bilateral cumulative radon concentration were obtained, and relevant software was used to obtain the single-sided k of the fitting slope before noise reduction, and then the radon exhalation rate of the uranium-like rock samples was calculated in accordance with Formula (2). The calculation process is as follows:

$$J = \frac{k \cdot V_e}{S} \quad (2)$$

In Formula (2), J represents the radon exhalation rate of the sample, $Bq \cdot m^{-2} \cdot s^{-1}$; k represents the slope of the fitting curve of the radon exhalation of the sample, $Bq \cdot m^{-3} \cdot s^{-1}$; S represents the bottom area when the sample is exposed, m^2; and V_e represents the effective volume in the radon collection volume except for the sample, m^3.

Based on the law of radon diffusion and migration, the measurement method is as follows:

Radon concentration measurement: Place the sample in a sealed container and monitor the radon concentration within the container over time using a measurement system like RAD7, recording the cumulative values.

Calculation of correction parameters: Fit the fitting slope k before noise reduction with relevant software. Its unit is $Bq \cdot m^{-3} \cdot s^{-1}$.

Determination of volume and area: S is the exposed bottom area of the specimen, in units of m^2. V_e is the effective volume except the sample in the radon collection volume, and the unit is m^3.

3. Experimental Results and Discussion

3.1. Analysis of Fly Ash Properties

The results of the XRD analysis of fly ash are shown in Figure 1.

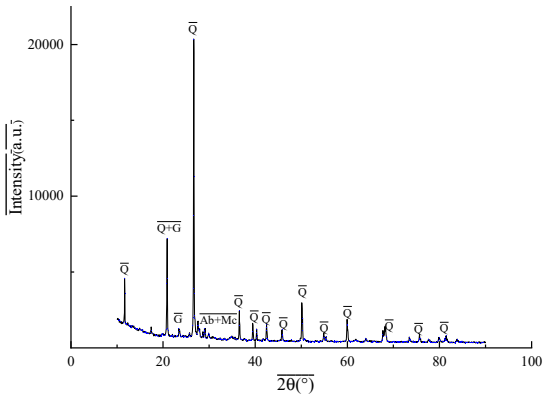

Figure 1. XRD patterns of fly ash samples.

It can be seen from Figure 1 that the phase composition of fly ash is mainly quartz, feldspar, kaolin minerals (such as bauxite), garnet, talc and so on. The characteristic diffraction peak of quartz is sharp, and the crystallinity is good, indicating that the content of quartz in fly ash is very high.

3.2. Scanning Electron Microscope Results

In this study, a Helios Nanolab 600i scanning electron microscope was used to analyze the micromorphology of uranium tailings. The distribution and morphological characteristics of minerals in uranium tailings were observed by scanning electron microscopy, and the shape and distribution of nano/micron pores in uranium tailings and the content of constituent elements were obtained. As shown in Figure 2(a), there was a whole rock

mass of uranium tailings. The rock mass is usually gray or brown, and the texture is rough. It includes other non-radioactive elements and minerals, such as quartz, feldspar, mica, etc. As shown in Figure 2b, when the particle size of each mineral is about 30 μm, the surface of quartz in uranium tailings is smooth and shows obvious grease luster, and a small amount of impurity particles with different particle sizes are attached to the surface of quartz. The surface of feldspar is rough, mainly composed of flake grains. Gypsum dihydrate is mainly lath-shaped, with a smooth surface and a small amount of impure particles. As shown in Figure 2c, the feldspar particles in uranium tailings include fine powder, and the particle size is usually below 10 μm. It presents a columnar structure with a clear axial growth direction. It also contains various inclusions and impurities, such as other mineral particles, bubbles or fissure fillings. As shown in Figure 2d, the dihydrate gypsum particles in uranium tailings include fine powder, and the particle size is usually below 10 μm. It can be seen from the scanning results that the dihydrate gypsum crystal presents a plate-like structure with a clear plane and edge.

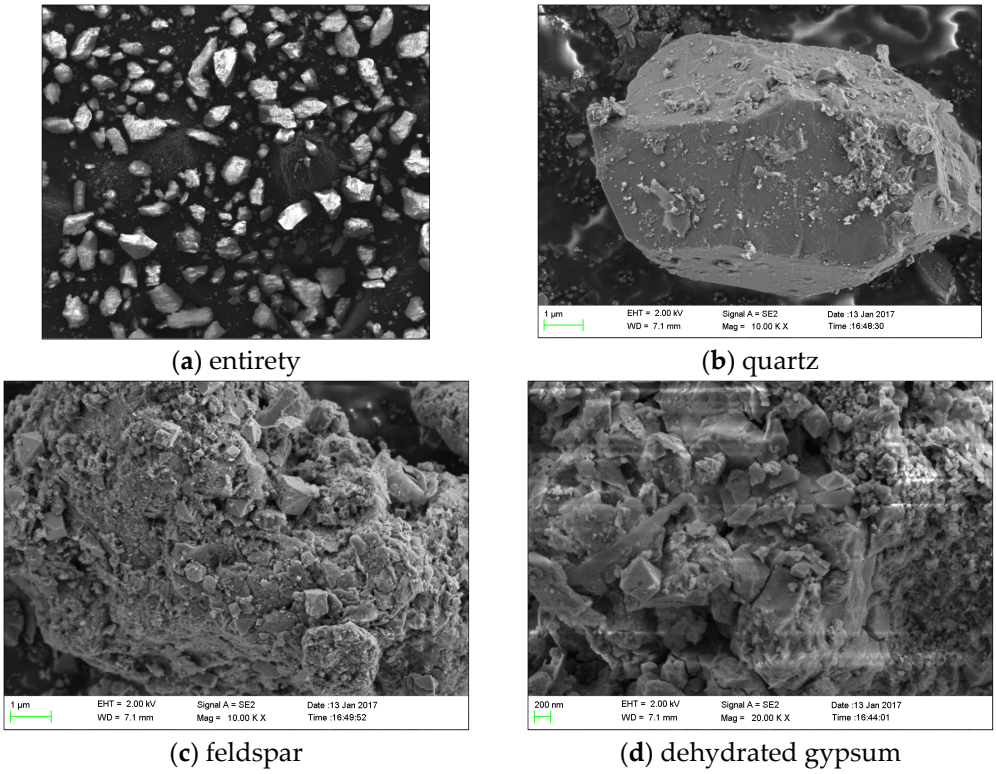

(**a**) entirety (**b**) quartz

(**c**) feldspar (**d**) dehydrated gypsum

Figure 2. SEM images of uranium tailing sample.

Then, the Helios nanolab 600i field emission scanning electron microscope was employed for the scanning of the original uranium tailings (Figure 2), and the solidified body mixed with different curing agents (blast furnace slag, lime and fly ash) and the scanning results (resolution was 1 μm) were obtained, as shown in Figure 3a–c.

From Figures 2 and 3, the original sample of uranium tailings can be seen. Figure 2 shows scattered accumulation before curing. After adding the curing agent, it was cemented together through the interactions of interlacing, filling and wrapping after chemical reaction, so that each sample shows a certain degree of cementation, but the degree of cementation was different with different dosages. In Figure 3a, when the content was 15%, the cementation degree of GBFS was the best, both samples of which were connected to each other, and there were fewer bulk deposits. The second curing agent was FA, of which most of the sample was connected together, but there was still a small part of the remainder uncemented. Finally, it was QL, which was cemented as a whole, but the unconnected parts were significantly more than those with GBFS or FA. Figure 3b,c are basically consistent

with Figure 3a. It is obvious in Figure 3a–c that with the increase in the content of the curing material, the better the degree of cementation and the better the degree of crystal form of the sample scanning results. Therefore, it can be concluded that the sample mixed with granulated blast furnace slag has the best curing effect, followed by fly ash and finally lime.

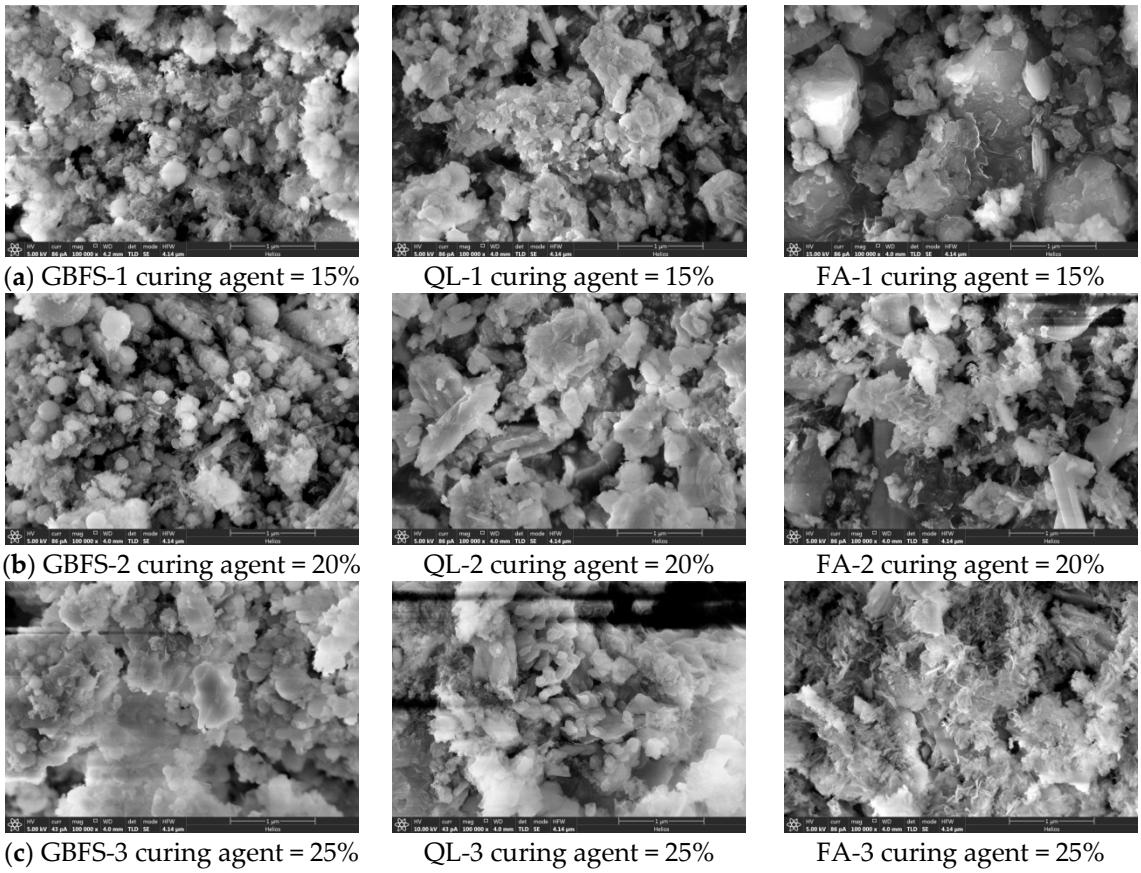

Figure 3. Scanning electron microscopy results of uranium tailings and samples mixed with different curing agents.

3.3. Permeability Coefficient Results

The permeability coefficient of the solidified uranium tailing body is a crucial indicator that reflects the seepage capacity of uranium tailings after undergoing solidification. It specifically measures the resistance of the solidified body to fluid flow, providing insights into its impact on fluid migration and diffusion in practical applications. This metric is essential for evaluating the sealing performance and long-term stability of the solidified uranium tailings. Its physical meaning is the permeability of the medium to a specific fluid. The permeability coefficient of uranium tailings in an undisturbed sand matrix is 5.58×10^{-3} cm·s^{-1}. The permeability coefficient values of other samples are shown in Figure 4.

The following can be seen from Figure 4:

(1) The permeability coefficient of the sample has a significant positive correlation with the amount of curing agent. The greater the amount of curing agent, the smaller the permeability coefficient. When the same dosage of different curing agents is 15%, 30% and 25%, the permeability coefficient values under the three curing dosages from large to small are quicklime (QL), fly ash (FA) and blast furnace slag (GBFS).

(2) Compared with the permeability coefficient of uranium tailings of 5.58×10^{-3} cm s^{-1} and the permeability coefficient in the field measured value of tailings dam [17], the permeability coefficient of each sample is smaller than the above three cases. More-

over, the trend of the permeability coefficient of each sample is a quadratic function: $Y = 0.013X^2 - 0.0196X + 0.778$.

(3) The porosity of each sample is smaller than that of the original sand. Among them, GBFS-3 has the best curing effect and the densest porosity, followed by FA-3 [18–22], and finally QL-3. This is consistent with the results of electron microscope scanning of each sample in the previous section.

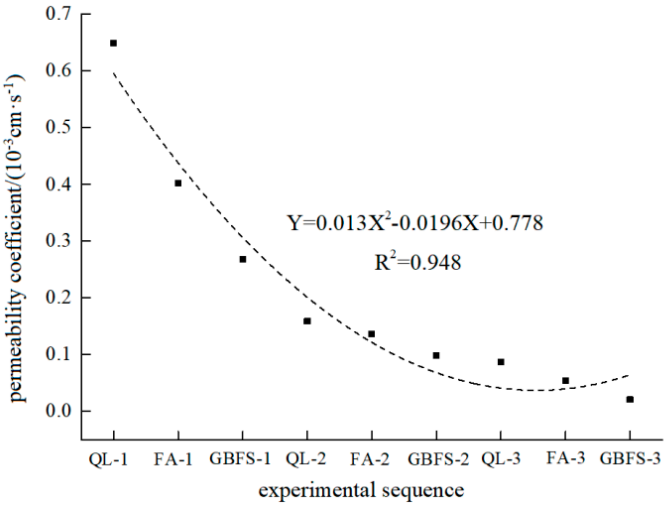

Figure 4. The permeability coefficient curve of each sample.

3.4. Measurement and Analysis of Radon Exhalation Rate

According to the law of the diffusion and migration of radon, the theoretical model in the relevant literature and the measured values of single-sided and double-sided cumulative radon concentration measured through experiments, using relevant software to obtain the fitting slope single-sided k, before noise reduction, the radon exhalation rate of uranium-like ore rock samples is to be calculated by means of Formula (2). At the same time [23,24], the previous measurement and analysis data are substituted into Formula (2) so that the radon exhalation rate of the sample can be determined. The specific results are presented in Figures 5 and 6.

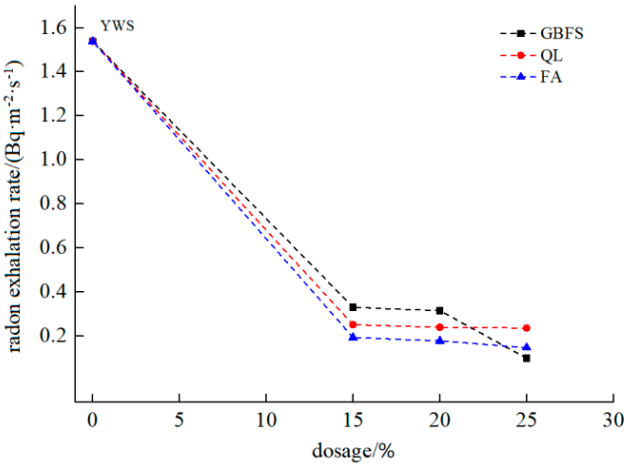

Figure 5. Uranium tailings and single-sided radon exhalation rate curve of each sample.

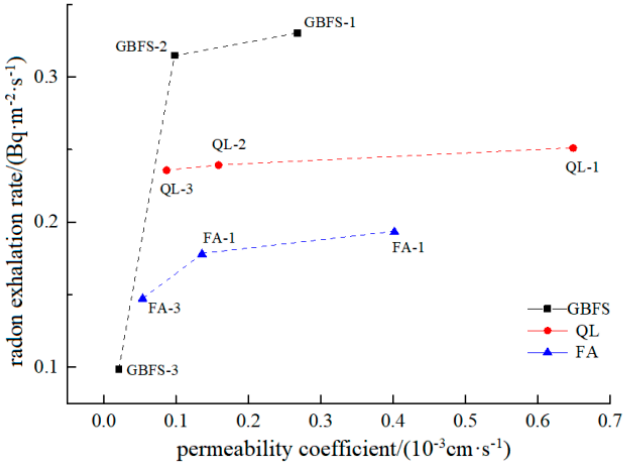

Figure 6. Relationship between permeability coefficient and radon exhalation rate of each sample.

From Figures 5 and 6, the following can be observed:

(1) The radon exhalation rate of uranium tailings' undisturbed sand in a uranium tailing pond is 1.5377 Bq·m^{-2}·s^{-1}. The radon exhalation rate of the uranium tailing solidified samples mixed with three solidified materials meets the requirements of China's medium- and low-radioactive waste (GB 23727-2009) after decommissioning and treatment, and the radon exhalation rate is not more than 0.74 Bq·m^{-2}·s^{-1}.

(2) It can be observed from Figure 5 that with the increase in the content of curing materials, the radon exhalation rate of each sample gradually decreases, but the decrease is not obvious. Figure 6 shows the relationship between the radon exhalation rate and permeability coefficient of nine kinds of samples. The decreases in the radon exhalation rate from large to small correspond to blast furnace slag, fly ash and then quicklime.

(3) With a comprehensive analysis of the results of scanning electron microscopy, the permeability coefficient and radon exhalation rate of each sample show that the smaller the permeability coefficient value, the better the degree of the mineral cementation of the microscopic scanning results, which reduces the pores in the sample, resulting in a reduction in the migration channel after radon exhalation in the sample and finally leads to a reduction in radon exhalation rate of each sample.

4. Conclusions

To evaluate the permeability coefficient and radon reduction effectiveness of uranium tailings solidified with three different materials, a comprehensive series of experimental studies were conducted. Initially, samples were prepared using various curing agents through a methodical process that included batching, mixing, vibrating, and curing. Each of these steps was carefully controlled to ensure consistent and reliable results. Following sample preparation, the uranium tailings and each sample were tested for permeability coefficient and scanning electron microscopy. According to the analysis of the test results, the following conclusions can be drawn:

(1) Through the X-ray diffraction (XRD) composition identification and analysis of uranium tailings, it was concluded that the main components of uranium tailings are quartz, dihydrate gypsum, albite and microcline. The proportions of the specific components are as follows: quartz: 45%; dihydrate gypsum: 15%; albite: 20%; plagioclase: 20%.

(2) The amount of curing agent and the different addition of curing agent have a significant effect on the permeability coefficient of the sample. In taking the same dosages of 15%, 20% and 25% of different curing agents as an example, the more curing agent content, the smaller the permeability coefficient of the sample and the better the cementation degree of the scanning electron microscope. At the same time, among the three curing agents, the material that affects the permeability coefficient and leads to smaller pores is blast furnace slag, followed by fly ash, and finally quicklime.

(3) The permeability coefficient of each sample shows a quadratic function relationship, and its expression is $Y = 0.013X^2 - 0.0196X + 0.778$. At the same time, the reductions in the permeability coefficient and radon exhalation rate of each sample are basically consistent with the results obtained by SEM. That is, the better the cementation degree of each sample, the smaller the permeability coefficient and radon exhalation rate.

Author Contributions: Conceptualization, J.W.; methodology, J.W.; formal analysis, J.W.; resources, S.Z.; data curation, J.W. All authors have read and agreed to the published version of the manuscript.

Funding: This research was funded by the Opening Project of Cooperative Innovation Center for Nuclear Fuel Cycle Technology and Equipment, University of South China 2019KFY25 and Key Laboratory of Advanced Nuclear Energy Design and Safety, Ministry of Education (KLANEDS202320).

Data Availability Statement: The raw data supporting the conclusions of this article will be made available by the authors on request.

Conflicts of Interest: The authors declare no conflicts of interest.

References

1. Jia, L. Fundamental Research on the High Performance Concrete Made by Iron Tailings and Iron Barren Rocks. Master's Thesis, University of Science and Technology Beijing, Beijing, China, 2015.
2. Liandong, L.; Zhigang, F.; Qiang, M. Study on the occurrence form and activity of uranium in Hunan uranium tailings. *Environ. Pollut. Control.* **2014**, *36*, 11–14.
3. Liandong, L. Experimental Study of a Uranium Tailings in Hunan Uranium Activity and Fixed. Master's Thesis, University of South China, Hengyang, China, 2014.
4. Shanggeng, L. *Treatment and Disposal of Radioactive Wastes*; China Environmental Science Press: Beijing, China, 2007.
5. Peng, W.; Xianjun, L.; Shugang, H. Study Progress of the Activation of Granulated Blast Furnace Slag Cementitious Material. *Met. Mine* **2012**, *436*, 157–161.
6. Yaolin, Y.; Xuewen, Q.; Zong, Z. Utilization of GGBS in stabilization of soft soils and its mechanism. *Chin. J. Geotech. Eng.* **2013**, *35* (Suppl. S2), 829–833.
7. Ahmed, A. Compressive strength and microstructure of soft clay soil stabilized with recycled bassanite. *Appl. Clay Sci.* **2015**, *104*, 27–35. [CrossRef]
8. Yadu, L. Stabilization of soft soil with granulated blast furnace slag and fly ash. *Int. J. Res. Eng. Technol.* **2013**, *2*, 115–119.
9. Dana, K.; Dey, J.; Das, S.K. Synergistic effect of fly ash and blast furnace slag on the mechanical strength of traditional porcelain tiles. *Ceram. Int.* **2005**, *31*, 147–152. [CrossRef]
10. Aperador, W.; Delgado, A.; Bautista-Ruiz, J. Effect of durability and chloride ion permeability in ternary cementitious concrete with additions of fly ash and blast furnace slag. *Int. J. Electrochem. Sci.* **2016**, *11*, 2297–2305. [CrossRef]
11. Chi, M.; Chang, J.J.; Yeih, W. Effects of Circulated Fluidized-Bed Fly Ash, Ground Granulated Blast-Furnace Slag and Coal Fly Ash on Properties of Mortars. In Proceedings of the International MultiConference of Engineers and Computer Scientists 2017, Hong Kong, China, 15–17 March 2017.
12. Yuan, W. Optimization Research for Stabilization Schemes of Soft Soils in Hefei Lakeside. Ph.D. Thesis, Anhui Jianzhu University, Hefei, China, 2015.
13. Qi, T. Mechanical Characteristics and Mechanisms of Dredeged Silt Soildified by Fly Ash and Slag. Ph.D. Thesis, North China University of Science and Technology, Qinhuangdao, China, 2015.
14. Ye, Y.; Zhao, Y.; Wang, L.; Cao, Y.; Fan, N.; Ding, D. Experimental Study on Radon Exhalation Rule of Heap-leaching Uranium Ore Heap. *At. Energy Sci. Technol.* **2015**, *49*, 187–192.
15. Ruoyun, M.; Lei, Z.; Qiuju, G. Study on accurate measurement of ^{220}Rn activity concentration by using RAD7 radon monitor. *At. Energy Sci. Technol.* **2012**, *46*, 1397–1401.
16. Lei, X.; Zhang, L.; Guo, Q. Comparison of closed chamber methods for accurate measurements of radon exhalation rates from building materials. *Radiat. Prot.* **2011**, *31*, 13–16+22.
17. Yin, G.Z.; Jing, X.F.; Wei, Z.A.; Li, X.S. Study of model test of seepage characteristics and field measurement of coarse and fine tailings dam. *Chinese J. Rock Mech. Eng.* **2010**, *29* (Suppl. S2), 3710–3718.
18. Huang, W.K.; Xie, Y.S.; Wang, Z.Q.; Zhu, Y.; Guo, Q.S.; Han, S.L.; He, H.Y.; Liu, S.; Sui, Q.L.; Ai, G.L. Quantified structural characteristics of granite and their constraints on radon exhalation. *J. Radioanal. Nucl. Chem.* **2024**, *333*, 6193–6212. [CrossRef]
19. Khyalia, B.; Yadav, J.; Kumar, N.; Dhiman, R.; Chauhan, R.P.; Parkash, R.; Dalal, R. Measurement and mapping of radon exhalation rate around the uranium mines in Sikar, Rajasthan, India. *J. Radioanal. Nucl. Chem.* **2024**, *333*, 5881–5888. [CrossRef]
20. Wu, J.; Xie, R.; Yi, H.; Hu, T.; Sun, J.; Liu, Z.; Li, H.; Liu, S.; Yuan, S.; Tan, Y. Laboratory study on the relationship between the vertical distribution of radon concentration in soil and the exhalation rate of radon from the soil surface. *J. Radioanal. Nucl. Chem.* **2024**, *333*, 6149–6154. [CrossRef]

21. Moreno, P.; Noverques, A.; Juste, B.; Sancho, M.; Verdú, G. Comparative analysis of techniques for estimating radon exhalation from building materials Radiation. *Phys. Chem.* **2024**, *46*, 734–735.
22. Liu, K.; Liu, Y.; Hong, C.; Xu, Z. Research on the influence of surface crack development on radon exhalation in uranium tailing ponds under wet and dry cycles. *J. Environ. Radioact.* **2024**, *278*, 107469. [CrossRef]
23. Ye, Y.; Shang, S.; Zhang, Y. Theoretical model for calculating and adjusting radon activity concentration in ventilation networks of uranium mines considering pressure drop effect. *J. Environ. Radioact.* **2024**, *276*, 107440. [CrossRef] [PubMed]
24. Ding, R.; Sun, Q.; Jia, H.; Xue, S.; Shi, Q. Study on the pore structure and radon release characteristics of coal in northern China. *Sci. Total Environ.* **2022**, *844*, 157148. [CrossRef]